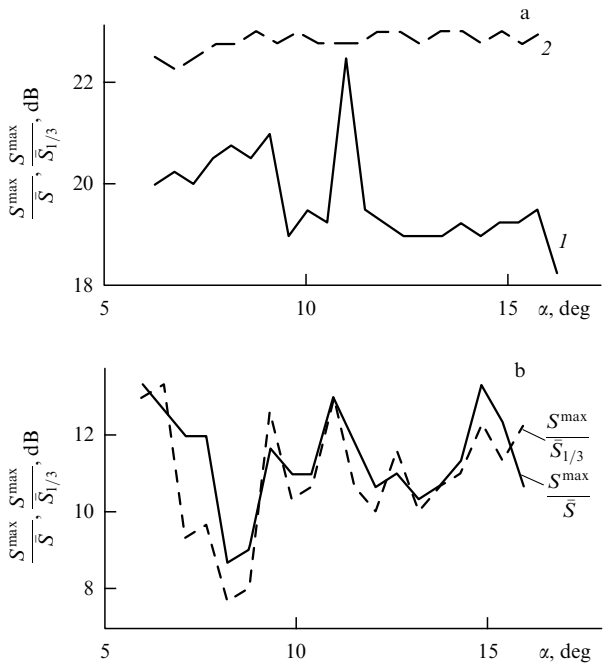

Figure 4. (a) The ratio of the amplitudes of global maximums $S^{\max}$ to the average levels of the envelopes $S(t)$ as a function of the irradiation angle α in response to irradiation by a reference signal: *1*, $S^{\max}/\bar{S}$ as a function of α; *2*, $S^{\max}/\bar{S}_{1/3}$ as a function of α. (b) The ratio of the amplitudes of global maximums $S^{\max}$ to the average levels of the envelopes $S(t)$ as a function of the irradiation angle α in response to irradiation by a train of seven equidistant pulses.

formed). Figure 4a gives an example of this dependence on the irradiation angle for a body in the horizontal plane, $\alpha = 5-15°$; the reference signal was formed in the irradiation of the body at $\alpha_0 = 10°$. Figure 4b gives an example of these curves for irradiation of the same body with seven equidistant pulses [the number of maximums in $S_\Sigma(t)$ is also roughly equal to 7]. These curves were plotted for probe pulses of equal length and for equal ranges of the body irradiation angle. On average, the ratios $S^{\max}/\bar{S}_{\Sigma_{1/3}}$ were greater than $S^{\max}/\bar{S}_\Sigma$, but the difference was insignificant. A comparison of the plots shown in Figs 4a and b demonstrates that the ratios $S^{\max}/\bar{S}_\Sigma$ and $S^{\max}/\bar{S}_{\Sigma_{1/3}}$ obtained for irradiation by reference signals at all angles were greater than the values in the case of equidistant pulses, which corresponds to irradiating a body with an extraneous reference signal. In this case, correct identification was faultless at all irradiation angles.

With this approach, the problem of identification is greatly simplified and in fact reduces to the problem of locating the global maximum. The price paid for increasing the noise immunity under multialternative identification is the need to send several reference signals whose number equals that of the bodies to be recognized. If reference signals are sent, the total information on the distribution of reference values $\{\tau_j\}$, incorporated in the conditional probability densities $f(\bigcup_{i=1} \tau_j)$, is not used. However, identification can be achieved by using the optimal criterion.

The suggested method is most convenient for identification of a known body against a background of noise and reverberation interference and in identifying complex-shape bodies in a multipath environment. Multipath propagation of signals in marine environments produces not one but several maxima $S_\Sigma^{\max}$ on $S_\Sigma(t)$ (depending on the hydrological environment). However, the procedure for identifying complex-shape bodies does not change in this case.

References

1. Davydov V S "Algoritm vyyavleniya sushchestvennykh maksimumov v ogibayushchei signala" ("Algorithm of identifying significant maximums on the signal envelope"), in *Modeli, Algoritmy, Prinyatie Reshenii: Tezisy 2-go Vsesoyuz. Akusticheskogo Seminara (10–14 Okt. 1988, Leningrad)* (Models, Algorithms, Decision Making: Abstracts of 2nd USSR Acoustic Seminar (Oct. 10–14, 1988, Leningrad)) (Moscow: N.N. Andreev Acoustic Inst., USSR Acad. Sciences, 1988) p. 65
2. Bondar L F, Davydov V S "Issledovanie funktsii raspredeleniya priznakov, primenyaemykh dlya raspoznavaniya podvodnykh skal i donnykh gruntov" ("Distribution functions of attributes used for identifying underwater rocks and bottom soil"), in *Trudy 9-i Vsesoyuz. Konf. po Informatsionnoi Akustike (Mart 1985 g.)* (Proc. of the 9th USSR Conf. on Information Acoustics (March 1985)) (Moscow: N.N. Andreev Acoustic Inst., USSR Acad. Sciences, 1987) p. 98
3. Davydov V S "Issledovanie statisticheskikh svoistv impul'snukh posledovatel'nostei, obuslovlennykh gruppoi zhestko svyazannykh otrazhatelei" ("Statistical properties of pulse sequences prepared for a group of rigidly connected reflectors), in *Obrabotka Akusticheskoi Informatsii v Mnogokanal'nykh Sistemakh* (Processing of Acoustic Information in Multichannel Systems) Issue 15 (Ed. V V Rotin) (Leningrad: Sudostroenie, 1988) p. 41
4. Davydov V S *Raspoznavanie v Gidrolokatsii* (Identification and Recognition in Hydrolocation) (St.-Petersburg: SPbGTEU 'LETI', 2005)
5. Davydov V S "Optimal'noe reshayushchee pravilo dlya raspoznavaniya tel slozhnoi geometricheskoi formy po otrazhennym gidroakusticheskim signalam" ("Optimum decision rule for identification of bodies of complex geometric shapes using reflected hydroacoustic signals"), in *Chelovek i Okean: Trudy Dokladov IV Dalnevostochnoi Konf. "Akusticheskie Metody i Sredstva Issledovaniya Okeana* (Man and the Ocean: Proc. of the IVth Far East Conf. "Acoustic Methods and Techniques for Ocean Research) (Vladivostok: AN SSSR, Far Eastern Research Center, 1986) p. 32
6. Davydov V S "Povyshenie pomekhozashchishchennosti raspoznavaniya tel slozhnoi formy po otrazhennym akusticheskim signalam" ("Increasing noise immunity of identification of bodies of complex shapes by using reflected acoustic signals") *Tekh. Akust.* **3** (1–2 (7–8)) 59 (1994)

PACS numbers: **12.20.–m**, 12.20.Ds, 31.30.Gs, 31.30.Jv
DOI: 10.1070/PU2008v051n11ABEH006801

Quantum electrodynamics of heavy ions and atoms: current status and prospects

V M Shabaev

1. Introduction

Quantum electrodynamics (QED), whose underlying principles were formulated by Dirac, Heisenberg, Born, Fock, Pauli, Wigner, Jordan, Fermi, and others by the early 1930s, has been quite successful in describing the emission (absorption) of a photon by an atom and the creation (annihilation) of electron–positron pairs, but second-order perturbative QED calculations yielded infinite results for some effects. This problem remained unsolved until about the late 1940s, when experiments by Lamb and Rutherford revealed what is now known as the Lamb shift, the splitting of the 2s and $2p_{1/2}$ energy levels in the hydrogen atom. Because there was virtually no doubt about the quantum-electrodynamic origin of the Lamb shift, this discovery paved the way to the solution

to the problem of singularities. The Lamb shift was first estimated by Bethe, and the modern theory of quantum electrodynamics, which solved the problem of infinities via the renormalization procedure, was developed by Dyson, Feynman, Tomonaga, and Schwinger. Because of the presence of a small parameter (the fine structure constant $\alpha \approx 1/137$), QED calculations rely on the perturbation theory, in which the Feynman diagram representation of each term enables formulating simple rules for writing formal mathematical expressions.

Until about the early 1980s, the only atoms that allowed testing QED were light ones such as hydrogen, positronium, helium, and muonium. For these, in addition to α, there is a small parameter αZ, where Z is the nucleus charge. For this reason, QED calculations for light atoms were limited to the few lowest orders in α and αZ, and comparison of theory and experiment only allowed testing the QED in the lowest orders in these parameters. This being a rather narrow testing range, the question naturally arises as to how to extend it. The immediate answer seems to be to go to higher orders in αZ to investigate QED effects for inner electrons in heavy neutral atoms (for example, the uranium atom), which are known to be in a strong (nonscreened) Coulomb field of the nucleus and for which the parameter αZ is not small. But the uncertainty in correlation effects, which usually is at or even exceeds the level of QED contributions, places strong accuracy constraints on the theoretical calculation of such systems. For this reason, heavy neutral atoms are usually treated only by means of the Breit equation, in which relativistic correlation effects are taken into account only approximately. The unique possibility of testing QED to all orders in terms of αZ has occurred with the advent of high-precision experiments on heavy multiply charged ions (such as hydrogen-like [1] or lithium-like [2–4] uranium ions) in which, on the one hand, αZ is not small (in uranium, $\alpha Z \approx 0.7$) and, on the other hand, because of the small number of electrons, correlation effects (i.e., electron–electron interaction effects) can be calculated to a high accuracy. It is the theory of such systems that occupies the bulk of this talk. As regards heavy neutral atoms, our discussion is brief and limited to recent advances in calculating QED corrections to spatial parity violation effects in neutral cesium (these corrections are very important for testing the Standard Model (SM) at low energies).

Relativistic units $\hbar = c = 1$ are used throughout the talk.

2. Binding energies of heavy ions

Because the number of electrons in a multiply charged ion is much smaller than the nucleus charge Z and because, therefore, the electrons interact much more strongly with the nucleus than with one another, a reasonable first approximation is that they do not interact at all and obey the one-electron Dirac equation in the Coulomb field $V_C(r)$ of the nucleus,

$$\big(\boldsymbol{\alpha}\mathbf{p} + \beta m + V_C(r)\big)\psi(\mathbf{r}) = E\psi(\mathbf{r})\,. \tag{1}$$

For a point-like nucleus, the Dirac equation is solved analytically. For a finite-size nucleus, both numerical and analytic solutions can be obtained [5].

QED corrections and those for the electron–electron interaction are included perturbatively. The corrections for the electron–electron interaction are suppressed by the parameter $1/Z$, which for heavy ions is comparable to the QED correction parameter α. Therefore, in the case of heavy ions, all the contributions are more conveniently characterized by the single parameter α. We note that unlike for light atoms, calculations for heavy atoms should be carried out without expanding in αZ.

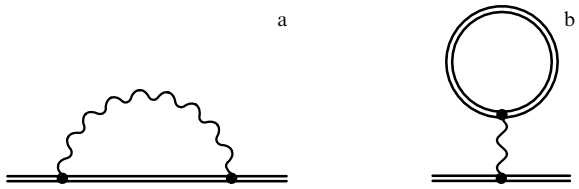

Figure 1. First-order one-electron diagrams: self-energy and vacuum polarization.

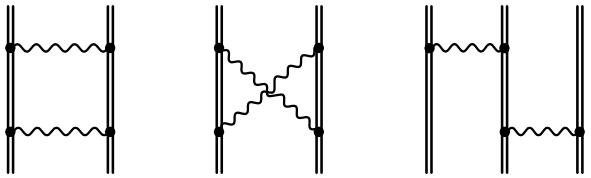

Figure 2. Two-photon exchange diagrams.

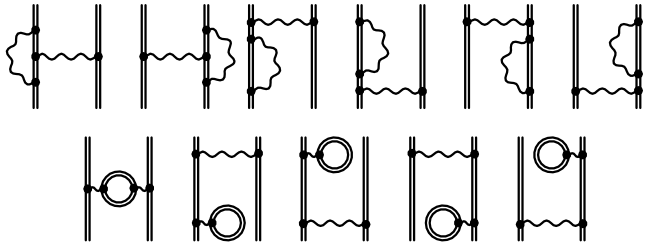

Figure 3. Screened-self-energy and vacuum polarization diagrams.

Because the electron mass is much smaller than the mass of the nucleus, most contributions can be calculated in the approximation of an infinitely heavy nucleus, when the nucleus simply serves as a source of an external Coulomb field and we are dealing with quantum electrodynamics in the Furry picture. First-order calculations in α should be done for contributions from the self-energy (Fig. 1a) and vacuum polarization (Fig. 1b) diagrams. For ions with two or more electrons, the one-phonon exchange diagram should of course also be included, and is rather easy to calculate. The main technical problem with calculating the self-energy and vacuum polarization diagrams is working without expanding in αZ. The first such calculations were performed in Ref. [6] for the self-energy diagram and in Refs [7, 8] for the vacuum polarization diagram.

The next stage in performing calculations in the Furry picture is to evaluate the contributions from second-order two- and three-electron diagrams, which include two-photon exchange diagrams (Fig. 2), as well as screened self-energy and vacuum polarization diagrams (Fig. 3). For this, the first thing to do is to derive the necessary calculation formulas. This problem mainly refers to the so-called reducible diagrams, i.e., those in which the total energy of an intermediate state of the atom equals the unperturbed energy of the reference state; for the remaining (irreducible) diagrams, the derivation poses no difficulty. In the late 1980s,

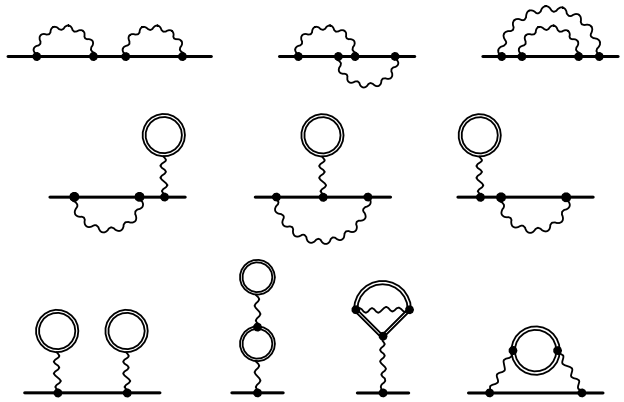

Figure 4. Second-order one-electron diagrams.

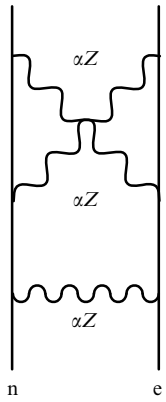

Figure 5. Typical diagram for the electron – nucleus interaction.

when the calculation of these diagrams was of particular topical interest, it was found that the adiabatic S-matrix formalism of Gell-Mann and Low, the most common approach at the time, has a number of drawbacks that make it computationally impractical. These include, among others, prohibitive technical difficulties in treating reducible diagrams, the lack of the renormalizability proof, the impossibility to calculate the energies of quasidegenerate states, and the unavailability of any analogous method capable of calculating transition amplitudes. All of these problems were overcome by using the method of two-time Green's functions developed for this purpose in Ref. [9] (see Ref. [10] for a detailed description). In particular, this method has been used to solve, for the first time, the computationally most challenging problem of deriving an expression for two-electron two-photon exchange diagrams [9]. In Ref. [11], this expression was calculated numerically for the ground state of helium-like atoms without expanding in αZ. Screened self-energy and vacuum polarization diagrams were calculated in Refs [12 – 14], followed by calculations for lithium-like ions [15] and for the excited states of helium-like atoms [16]. Recently, the full set of diagrams shown in Figs 2 and 3 were finally calculated for the $2p_{3/2}-2p_{1/2}$ transition for the boron-like argon ion [17].

Referring to the second-order one-electron diagrams in Fig. 4, calculations for some of these reduce to calculating first-order diagrams. An example is given by the diagrams shown in the second row of the figure, where the calculation reduces to the ordinary one-loop self-energy calculation for an effective potential composed of the Coulomb potential of the nucleus plus the vacuum polarization potential. At the same time, two-loop self-energy diagrams (seen in the first row of Fig. 4) pose challenging technical difficulties for calculation, as also do the last two diagrams in the figure. Considerable progress in this area was made in the relatively recent study in Refs [18, 19], where the full set of two-loop self-energy diagrams was calculated.

In these calculations, the nucleus is treated as an infinitely massive source of an external Coulomb field. Going beyond this approximation requires taking the finite mass of the nucleus, that is, the recoil effect, into account. In the nonrelativistic theory of a hydrogen-like atom, it is known that the recoil effect of the nucleus is readily taken into account by introducing the reduced electron mass $\mu = mM/(m+M)$. But this is not the case in the relativistic theory, which can only be formulated in the QED framework. A fully relativistic theory accounts for the nuclear recoil effect by considering all the diagrams for the electron – nucleus interaction via photon exchange. A typical example of such a diagram is shown in Fig. 5. The fact that each photon line in this diagram contributes a factor αZ explains the fundamental difference in how the theory accounts for the recoil effect in light and heavy atoms. For light (small-αZ) atoms, a calculation with only a few lowest-order diagrams is a sufficient approximation, but for heavy ions, in which the parameter αZ is not small, no finite number of diagrams suffice and, instead, the infinite sequence of such diagrams must be summed (at least in the first order in m/M). Because the standard QCD formalism offers no recipes for doing this, we are faced with a serious conceptual problem here. Reference [20] was the first to set out to derive a closed expression accurate to all orders in αZ for the nuclear recoil effect. The next important development in this area was the demonstration in Ref. [21] of the summability of the infinite sequences of diagrams of interest here. Full closed formulas for recoil corrections, accurate in the first order in m/M and exact in αZ, were obtained by the quasipotential method in Ref. [22]. According to these formulas, the recoil correction to the energy of the bound state a of a hydrogen-like atom is the sum of the lower and higher (in αZ) contributions,

$$\Delta E_{\mathrm{L}} = \frac{1}{2M}\left\langle a\right|\left[\mathbf{p}^2 - \left(\mathbf{D}(0)\,\mathbf{p} + \mathbf{p}\,\mathbf{D}(0)\right)\right]\left|a\right\rangle, \tag{2}$$

$$\Delta E_{\mathrm{H}} = \frac{\mathrm{i}}{2\pi M}\int_{-\infty}^{\infty}\mathrm{d}\omega\left\langle a\right|\left(\mathbf{D}(\omega) - \frac{[\mathbf{p}, V_{\mathrm{C}}]}{\omega + \mathrm{i}0}\right)G(\omega + E_{\mathrm{a}}) \times \left(\mathbf{D}(\omega) + \frac{[\mathbf{p}, V_{\mathrm{C}}]}{\omega + \mathrm{i}0}\right)\left|a\right\rangle. \tag{3}$$

Here, $\mathbf{p}$ is the momentum operator, $G(\omega)$ is the relativistic Coulomb Green's function, $D_m(\omega) = -4\pi\alpha Z\alpha_l D_{lm}(\omega)$, and $D_{ik}(\omega, r)$ is the transverse part of the Coulomb gauge photon propagator. We note that the scalar product is understood in Eqn (3). Reference [23], also relying on the quasipotential method, extended these formulas to atoms with several electrons. In later studies [24], other methods were used to derive formulas (2) and (3). The first numerical calculations with these formulas were performed in Ref. [25].

It is necessary, finally, to account for the polarization of the nucleus by the electron. This effect is represented by the diagrams of the two-photon exchange between the nucleus and an electron in which intermediate (virtual) states of the

Table 1. Energy of the $2p_{1/2}-2s$ transition in the Li-like uranium ion.

	Energy, eV
Breit approximation	322.13(7)
QED contributions of the first order in α	−42.93
QED contributions of the second order in α	1.55(7)
Nuclear recoil	−0.07
Nuclear polarization	0.03(1)
Full theoretical value	280.71(10)
Experimental value [4]	280.645(15)

nucleus are excited. Given that the internucleon interaction is understood only phenomenologically, calculating nuclear polarization is a serious physical problem, and it is in fact the errors from this calculation that determine the upper-bound accuracy of the full theoretical values needed. Calculations of this effect for heavy hydrogen-like ions were carried out in Refs [26, 27].

To date, the highest level of precision has been achieved in experiments to measure transition energies in lithium-like ions [2–4]. Table 1 shows the values of different contributions to the $2p_{1/2}-2s$ transition energy and compares the full theoretical value with the experimental result. The contribution due to the finite size of the nucleus is calculated for a Fermi nuclear charge distribution with account for the nuclear deformation [28]. It is seen that as far as lithium-like uranium is concerned, the current theory and experiment provide about a 0.2% test of QED in a strong Coulomb field.

3. Hyperfine structure

A number of high-precision measurements are available for determining the hyperfine ground state splitting of heavy hydrogen-like ions [29–32]. The primary motivation behind these measurements was the fact that in a heavy ion with nonzero nuclear spin, each electron experiences, in addition to the strong Coulomb field, a very strong magnetic field created by the magnetic moment of the nucleus; this a situation provides a unique opportunity for testing QED in the combination of the highest currently achievable electric and magnetic fields. The first such experiment was carried out on bismuth [29] and yielded the value 5.0840(8) eV for the hyperfine ground state splitting of the H-like ion $^{209}Bi^{82+}$. The theoretical value of the hyperfine splitting is conveniently written as

$$\Delta E = \Delta E_{\mathrm{Dirac}}(1-\varepsilon) + \Delta E_{\mathrm{QED}}\,, \tag{4}$$

where the Dirac value includes relativistic effects and the nuclear charge distribution correction, ε is the (Bohr–Weisskopf) correction for the nuclear magnetic moment distribution, and ΔE_{QED} is the QED correction. Calculating $\Delta E_{\mathrm{Dirac}}$ is straightforward. The QED correction has also been calculated by several groups, leading to reasonably consistent results. The main problem consists in calculating the Bohr–Weisskopf correction, which, because of its high sensitivity to the nuclear model, almost entirely determines the full theoretical uncertainty. For the H-like ion of bismuth, a calculation within a one-particle model of the nucleus yields the hyperfine splitting 5.101(27) eV [33], a value that agrees with experiment but contains a large error. A more accurate calculation for a many-particle nuclear model [34] yields $5.111(-3,+20)$ eV, which is in disagreement with experiment. Finally, a semiempirical calculation using an experimental value of hyperfine splitting in muonic bismuth yielded 5.098(7) eV [35], about two standard deviations from the experimental value. The QED contribution to the given hyperfine splitting is about −0.030 eV and is in fact comparable to the error in the Bohr–Weisskopf correction. Although this fact prevents the tests of QED by directly comparing theoretical and experimental results for the hyperfine structure of hydrogen-like ions, it has been shown [36] that QED effects can be experimentally identified by using a certain particular difference between the hyperfine splitting of H- and Li-like ions of the same isotope,

$$\Delta' E = \Delta E^{(2s)} - \xi \Delta E^{(1s)}\,, \tag{5}$$

where ξ is chosen so as to cancel the Bohr–Weisskopf effect. It turns out that both the parameter ξ and the difference $\Delta' E$ itself are weakly sensitive to variations in the nuclear model and can therefore be calculated to high precision. With this approach, it will be possible to test QED at the level of a few percent if the hyperfine splittings are measured to an accuracy $\sim 10^{-6}$. Such experiments are currently underway in Germany and the UK in the framework of the HITRAP (Heavy Ion Trap) project. The first experimental data on the hyperfine splitting in Li-like bismuth were obtained at the Livermore National Laboratory in the USA.

4. *g*-factor of multicharged ions

Precision *g*-factor measurements of the H-like carbon ion in a Penning trap [37] have generated considerable interest in the calculation of this quantity. The measurements were so accurate that their total precision was mainly determined by uncertainties in the electron mass *m*, which enters the formula for the *g*-factor along with the experimentally measured cyclotron and Larmor frequencies. This implies that knowing the theoretical value of the *g*-factor to within the desired accuracy would enable the electron mass to be determined with an accuracy exceeding that of the then-accepted value of *m* by several times. At the time, the two factors that determined the error in the theoretical value were the non-calculated higher-order nuclear recoil contributions and the error from the numerical calculation of the one-loop self-energy. Efforts to reduce the former resulted in a closed relativistic formula for the nuclear recoil correction to the atomic *g*-factor. Specifically, the following formula was derived, in the first order in m/M and in all orders in αZ, for the contribution from the nuclear recoil effect to the *g*-factor of an H-like ion [38]:

$$\Delta g = \frac{1}{\mu_0 m_{\mathrm{a}}} \frac{\mathrm{i}}{2\pi M} \int_{-\infty}^{\infty} \mathrm{d}\omega \left[\frac{\partial}{\partial B} \left\langle a \right| \left[\mathbf{p} - \mathbf{D}(\omega) + e\mathbf{A}_{\mathrm{cl}} \right] \times G(\omega + E_{\mathrm{a}}) \left[\mathbf{p} - \mathbf{D}(\omega) + e\mathbf{A}_{\mathrm{cl}} \right] \left| a \right\rangle \right]_{B=0}. \tag{6}$$

Here, μ_0 is the Bohr magneton, m_{a} is the projection of the moment on the *z* axis, $e = -|e|$ is the electron charge, and $\mathbf{A}_{\mathrm{cl}} = [\mathbf{B} \times \mathbf{r}]/2$ is the vector potential of the homogeneous magnetic field **B** directed along the *z* axis. It is assumed that all quantities are calculated in the presence of a magnetic field. A numerical calculation using expression (6) was carried out in Ref. [39], and a calculation of the one-loop self-energy to the required accuracy was performed in Ref. [40]. All in all, the comparison of the theoretical and experimental values of the *g*-factor of H-like carbon reduced the error in the value of the electron mass by a factor of four. These results, along with relevant studies on H-like oxygen [41], formed the basis for a

new value of m as given in the most recent compilation of fundamental constants [42].

It is expected that the g-factors of multicharged ions up to $Z = 92$ can be experimentally determined in the very near future in the framework of the HITRAP project. For ions with nonzero spin, such experiments can be used to determine nuclear magnetic moments to within $\sim 10^{-6}$. As shown in Ref. [43], the fine structure constant can also be independently measured in this way.

5. QED corrections to the parity-violating 6s–7s amplitude in neutral Cs

The study of parity violation remains one of the major tools for testing the Standard Model electroweak sector at low energies [44]. The measurement of the parity-violating 6s–7s amplitude in neutral Cs to within 0.3% [45] required for both calculating new corrections to this amplitude and revising those contributions already calculated. As a result, more accurately accounting for correlation effects [46], combined with the Breit interaction [47, 48] and vacuum polarization [49] corrections, has led to a weak charge of the cesium ion, differing by 2σ from the SM prediction. It became clear that testing the SM requires a consistent QED calculation of self-energy corrections. The first estimates of this effect were made for the so-called 'mixing coefficients' of the s and p states, the coefficients being rather artificial entities in the QED context. Although both references gave similar results for the total (minus $-\alpha/2\pi$) binding QED correction [$-0.5(1)\%$ in Ref. [50] and $-0.43(4)\%$ in Ref. [51]), only a calculation of the total gauge-invariant set of self-energy corrections to the P-violating amplitude could answer the question of agreement or disagreement with the Standard Model. Such a calculation was carried out is Ref. [52], where it was assumed that a valence electron moves in an effective local potential constructed from the nonlocal Dirac–Fock potential. The result for the total binding QED correction was $-0.27(3)\%$, differing by a factor of two from previous estimates. Later, a similar result was obtained in Ref. [53], where a revision of the previous calculations in Refs [50, 51] was performed.

Combining the QED contribution with other contributions and comparing the resulting total amplitude with the averaged experimental value of the vector polarizability $\beta = 26.99(5)a_B^3$ (see Ref. [46] and the references therein), the weak charge of ^{133}Cs is found to be

$$Q_W = -72.65(29)_{exp}(36)_{th}\,, \qquad (7)$$

which is 1.1σ from the SM prediction $-73.19(13)$ [54].

6. Conclusion

In this paper, theoretical results of the quantum electrodynamics of multicharged ions are presented and compared with experimental data, identifying the study of transition energies in heavy multicharged ions as the area where the QED in strong electric fields has by now been most thoroughly tested. A study of how QED affects the hyperfine structure of heavy ions, which would mean testing QED in the simultaneous presence of strong electric and magnetic fields, is greatly complicated by large uncertainties in corrections due to the nuclear magnetic moment distribution. The considerable reduction in these uncertainties for a certain particular difference of hyperfine splittings in H- and Li-like ions raises hope that such testing will become possible when necessary experiments, both underway and planned, are completed. The high-precision measurements of the g-factors of multicharged ions and a corresponding theory that has been developed have already resulted in a more accurate value of the electron mass and are expected to be used in the very near future to test QED in an external magnetic field and to obtain high-precision values of nuclear magnetic moments. It can be expected that these studies will also enable an independent, high-precision determination of the fine structure constant in the near future.

Large errors in calculating correlation effects in heavy neutral atoms make these systems impractical for verifying QED. However, when particularly precise calculations are to be made (for example, in estimating parity violation in a neutral Cs atom), QED corrections should be included. Computational QED techniques that have been developed for multicharged ions with a few electrons proved to apply to such systems as well. From a theoretical standpoint, what currently limits the tests of the Standard Model in neutral atoms is errors in correlation effects. In this connection, the study of parity violation in multicharged ions [55], where the accuracy of calculation is not subject to such limitations, holds considerable promise.

This work was supported in part by the RFBR grant No. 07-02-00125 and by the INTAS-GSI grant No. 06-10000012-8881.

References

1. Gumberidze A et al. *Phys. Rev. Lett.* **94** 223001 (2005)
2. Schweppe J et al. *Phys. Rev. Lett.* **66** 1434 (1991)
3. Brandau C et al. *Phys. Rev. Lett.* **91** 073202 (2003)
4. Beiersdorfer P et al. *Phys. Rev. Lett.* **95** 233003 (2005)
5. Shabaev V M *J. Phys. B: At. Mol. Opt. Phys.* **26** 1103 (1993)
6. Mohr P J *Ann. Phys.* (New York) **88** 26 (1974)
7. Soff G, Mohr P J *Phys. Rev. A* **38** 5066 (1988)
8. Manakov N L, Nekipelov A V, Fainshtein A G *Zh. Eksp. Teor. Fiz.* **95** 1167 (1989) [*Sov. Phys. JETP* **68** 673 (1989)]
9. Shabaev V M *Teor. Mat. Fiz.* **82** 83 (1990) [*Theor. Math. Phys.* **82** 57 (1990)]; *Izv. Vyssh. Uchebn. Zaved. Ser. Fiz.* **33** (8) 43 (1990) [*Sov. Phys. J.* **33** 660 (1990)]
10. Shabaev V M *Phys. Rep.* **356** 119 (2002)
11. Blundell S A et al. *Phys. Rev. A* **48** 2615 (1993); Lindgren I et al. *Phys. Rev. A* **51** 1167 (1995)
12. Persson H et al. *Phys. Rev. Lett.* **76** 204 (1996)
13. Artemyev A N, Shabaev V M, Yerokhin V A *Phys. Rev. A* **56** 3529 (1997)
14. Yerokhin V A, Artemyev A N, Shabaev V M *Phys. Lett. A* **234** 361 (1997)
15. Artemyev A N et al. *Phys. Rev. A* **60** 45 (1999); Yerokhin V A et al. *Phys. Rev. A* **60** 3522 (1999); Yerokhin V A et al. *Phys. Rev. Lett.* **85** 4699 (2000); Sapirstein J, Cheng K T *Phys. Rev. A* **64** 022502 (2001); Andreev O Yu et al. *Phys. Rev. A* **67** 012503 (2003)
16. Artemyev A N et al. *Phys. Rev. A* **71** 062104 (2005)
17. Artemyev A N et al. *Phys. Rev. Lett.* **98** 173004 (2007)
18. Yerokhin V A, Indelicato P, Shabaev V M *Phys. Rev. Lett.* **91** 073001 (2003); *Zh. Eksp. Teor. Fiz.* **128** 322 (2005) [*JETP* **101** 280 (2005)]
19. Yerokhin V A, Indelicato P, Shabaev V M *Phys. Rev. Lett.* **97** 253004 (2006)
20. Labzovskii L N, in *Doklady 17-ogo Vsesoyuznogo Siezda po Spektroskopii, Minsk, 1971* (Proceedings of the 17th All-Union Congress on Spectroscopy, Minsk, 1971) Pt. 2 *Teoriya Atomnykh Spektrov* (Theory of Atomic Spectra) (Moscow, 1972) p. 89
21. Braun M A *Zh. Eksp. Teor. Fiz.* **64** 413 (1973) [*Sov. Phys. JETP* **37** 211 (1973)]
22. Shabaev V M *Teor. Mat. Fiz.* **63** 394 (1985) [*Theor. Math. Phys.* **63** 588 (1985)]
23. Shabaev V M *Yad. Fiz.* **47** 107 (1988) [*Sov. J. Nucl. Phys.* **47** 69 (1988)]

24. Yelkhovsky A S, Preprint No. 94-27 (Novosibirsk: Budker Inst. of Nucl. Phys., 1994); Pachucki K, Grotch H *Phys. Rev. A* **51** 1854 (1995); Shabaev V M *Phys. Rev. A* **57** 59 (1998); Adkins G S, Morrison S, Sapirstein J *Phys. Rev. A* **76** 042508 (2007)
25. Artemyev A N, Shabaev V M, Yerokhin V A *Phys. Rev. A* **52** 1884 (1995)
26. Plunien G, Soff G *Phys. Rev. A* **51** 1119 (1995); **53** 4614 (1996)
27. Nefiodov A V et al. *Phys. Lett. A* **222** 227 (1996)
28. Kozhedub Y S et al. *Phys. Rev. A* **77** 032501 (2008)
29. Klaft I et al. *Phys. Rev. Lett.* **73** 2425 (1994)
30. Crespo López-Urrutia J R et al. *Phys. Rev. Lett.* **77** 826 (1996); *Phys. Rev. A* **57** 879 (1998)
31. Seelig P et al. *Phys. Rev. Lett.* **81** 4824 (1998)
32. Beiersdorfer P et al. *Phys. Rev. A* **64** 032506 (2001)
33. Shabaev V M et al. *Phys. Rev. A* **56** 252 (1997)
34. Sen'kov R A, Dmitriev V F *Nucl. Phys. A* **706** 351 (2002)
35. Elizarov A A et al. *Nucl. Instrum. Meth. Phys. Res. B* **235** 65 (2005)
36. Shabaev V M et al. *Phys. Rev. Lett.* **86** 3959 (2001)
37. Häffner H et al. *Phys. Rev. Lett.* **85** 5308 (2000)
38. Shabaev V M *Phys. Rev. A* **64** 052104 (2001)
39. Shabaev V M, Yerokhin V A *Phys. Rev. Lett.* **88** 091801 (2002)
40. Yerokhin V A, Indelicato P, Shabaev V M *Phys. Rev. Lett.* **89** 143001 (2002)
41. Verdú J et al. *Phys. Rev. Lett.* **92** 093002 (2004)
42. Mohr P J, Taylor B N *Rev. Mod. Phys.* **77** 1 (2005)
43. Shabaev V M et al. *Phys. Rev. Lett.* **96** 253002 (2006)
44. Khriplovich I B *Phys. Scripta* **T112** 52 (2004)
45. Wood C S et al. *Science* **275** 1759 (1997); Bennett S C, Wieman C E *Phys. Rev. Lett.* **82** 2484; **83** 889 (1999)
46. Dzuba V A, Flambaum V V, Ginges J S M *Phys. Rev. D* **66** 076013 (2002)
47. Derevianko A *Phys. Rev. Lett.* **85** 1618 (2000)
48. Kozlov M G, Porsev S G, Tupitsyn I I *Phys. Rev. Lett.* **86** 3260 (2001)
49. Johnson W R, Bednyakov I, Soff G *Phys. Rev. Lett.* **87** 233001 (2001)
50. Kuchiev M Yu *J. Phys. B: At. Mol. Opt. Phys.* **35** L503 (2002); Kuchiev M Yu, Flambaum V V *Phys. Rev. Lett.* **89** 283002 (2002); *J. Phys. B: At. Mol. Opt. Phys.* **36** R191 (2003)
51. Milstein A I, Sushkov O P, Terekhov I S *Phys. Rev. Lett.* **89** 283003 (2002); *Phys. Rev. A* **67** 062103 (2003)
52. Shabaev V M et al. *Phys. Rev. Lett.* **94** 213002 (2005); *Phys. Rev. A* **72** 062105 (2005)
53. Flambaum V V, Ginges J S M *Phys. Rev. A* **72** 052115 (2005)
54. Rosner J L *Phys. Rev. D* **65** 073026 (2002)
55. Labzowsky L N et al. *Phys. Rev. A* **63** 054105 (2001)

PACS numbers: 06.20.Jr, 06.30.Ft, 12.20.Fv, 32.10.Fn, 32.30.Jc, 42.62.Fi
DOI: 10.1070/PU2008v051n11ABEH006644

High-precision laser spectroscopy of cold atoms and the search for the drift of the fine structure constant

N N Kolachevsky

1. Introduction

This review presents the main scientific results obtained over the last several years at the Laboratory of Active Media Optics of the Optical department of the Lebedev Physical Institute. The work was aimed at the search for and the investigation of high-finesse optical resonances in atomic ensembles. This allows carrying out sensitive tests of fundamental physical theories and opens the possibility of creating prospective frequency references in the optical range. A new laboratory method has been presented to search for the drift of the fine structure constant by using a frequency comb of a femtosecond laser, and sensitive experiments are being performed on testing the quantum electrodynamic theory. Work has started on laser cooling of the thulium atom, which experiences a narrow transition near 1.14 μm. The possibility of cooling was analyzed experimentally and theoretically, and the transitions most promising for the cooling were determined. A new generation of ultrastable optical cavities was developed for stabilizing the frequency of laser systems, which allows detecting optical resonances with a sub-Hertz resolution. A compact magneto-optical trap for rubidium atoms was created, and the interaction of femtosecond-laser radiation with a laser-cooled ensemble of atoms was investigated.

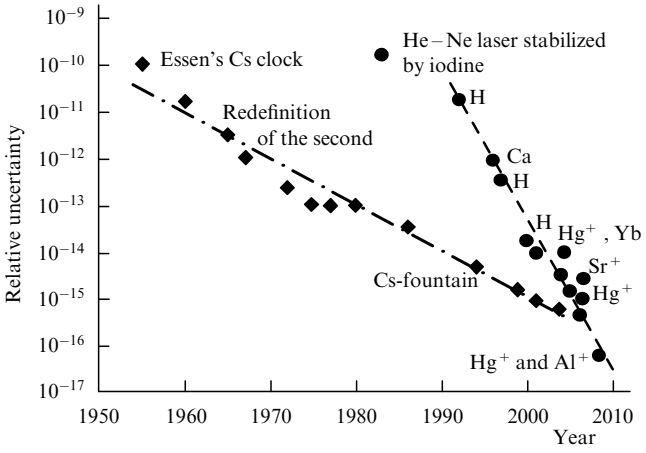

Figure 1. Uncertainty evolution for microwave (rhombs, dash-dotted line) and optical (circles, dashed line) frequency references. Noticeable progress in the development of optical standards is related to the evolution of new ultrastable laser systems, methods for measuring and comparing optical frequencies by means of an optical comb, and the development of new spectroscopic objects based on captured and cooled atoms and ions.

High-precision laser spectroscopy and laser cooling of atomic ensembles are rapidly developing fields of modern physics. In the last decade, the most impressive achievements have been awarded Nobel prizes for physics, specifically, the development of methods for cooling and trapping atoms by laser radiation (1997), the experimental discovery of Bose – Einstein condensation in dilute gases of alkali metals (2001), and the contribution to the development of methods for high-precision spectroscopy and the creation of a frequency comb on the basis of a femtosecond laser (2005) [1]. Intense investigations in the field of high-precision spectroscopy and metrology started about 30 years ago [2, 3]; however, it took a long time to approach the measurement uncertainty of $10^{-17} - 10^{-18}$, envisaged in pioneering works by A L Shavlov, V P Chebotaev, V S Letokhov, T W Hänsch, J L Hall, and other classics of nonlinear laser spectroscopy. As the result of long-term work, scientists from metrological and laser centers in the USA, Germany, Russia, France, England, and other countries succeeded in reducing the relative error of optical frequency references to 2×10^{-17} [4], which is by an order of magnitude better than the accuracy of the best primary standards, namely, cesium fountains [5]. In Fig. 1a, the relative errors of microwave and optical standards are compared.

Rapid progress in optical standards is mainly related to the development of simple-to-use laser systems with superior characteristics, which satisfy the most stringent requirements of experimenters. Laser systems are used for cooling and capturing atoms and ions in traps, for preparing their internal states, and in the spectroscopy of ultra-narrow 'clock'